Published in final edited form as:
J Immunol. 2011 February 1; 186(3): 1477–1485. doi:10.4049/jimmunol.1000454.

Plasmacytoid dendritic cell dichotomy: identification of interferon-α producing cells as a phenotypically and functionally distinct subset[#)]

Pia Björck[1),*], **H. Xianne Leong**[1)], and **Edgar G. Engleman**[1)]
[1)] Department of Pathology, Stanford University, Palo Alto, CA 94304, U.S.A

Abstract

Plasmacytoid dendritic cells (pDC) produce large amounts of type I interferon in response to invading pathogens, but can also suppress immune responses and promote tolerance. Here we show that in mice these functions are attributable to two distinct pDC subsets, one of which gives rise to the other. $CD9^{pos}$ Siglec-H^{low} pDC secrete interferon-α (IFN-α) when stimulated with Toll-like receptor (TLR) agonists, induce cytotoxic T lymphocytes (CTLs) and promote protective anti-tumor immunity. By contrast, $CD9^{neg}$ Siglec-H^{high} pDC secrete negligible amounts of IFN-α, induce FoxP3+ CD4+ T cells and fail to promote anti-tumor immunity. Although newly formed pDC in the bone marrow (BM) are $CD9^{pos}$ and are capable of producing IFN-α, after these cells traffic to peripheral tissues they lose CD9 expression and the ability to produce IFN-α. We propose that newly generated pDC mobilized from the BM, rather than tissue-resident pDC, are the major source of IFN-α in infected hosts.

Introduction

pDC are recognized as the main source of IFN-α after challenge with pathogens [1–3]. IFN-α, in turn, can directly activate natural killer (NK) cells, promote CTL activity, induce B cell antibody production and differentiation of myeloid DC (mDC) [1, 4]. However, there is now accumulating evidence that these cells also promote antigen-specific regulatory T cell activation, transplantation tolerance and oral tolerance [5–8]. Whether these opposing functions are mediated by distinct subpopulations of pDC or by a single cell type that can be reprogrammed in response to different stimuli is unknown.

Self-tolerance is critical for the avoidance of autoimmune disease, and a multiplicity of mechanisms exist in healthy individuals to assure its maintenance. The most important of these are felt to be central deletion of high-affinity autoreactive T cells in the thymus and suppression of excessive effector cell activity by regulatory T cells in the periphery [9]. However, these mechanisms may not suffice to prevent uncontrolled or excessive release of IFN-α from pDC, which can be activated by TLR agonists in the absence of T cells [1, 4]. As a highly pleiotropic cytokine, IFN-α production needs to be strictly regulated, as it may be directly involved in the pathogenesis and exacerbation of various autoimmune disorders [10–12].

[#)]Supported by the National Institute of Health (NIH) grant 5 RO1 AR051748-04.

[*]To whom correspondence should be sent: Pia Björck, Stanford University, Department of Pathology/Stanford Blood Center, 3373 Hillview Avenue, Palo Alto, CA 94304, U. S. A, bjorck@stanford.edu, phone: 650-723-7998, FAX: 650-725-4470.

Contribution: P.B designed and performed all experiments except PCR, and wrote the manuscript. XL performed the PCR experiments. E.G.E helped with discussions and with writing the manuscript.

Conflict-of-interest disclosure: The authors declare they have no competing financial interests.

In this study we show that a phenotypically and morphologically distinct subset of pDC is responsible for all, or nearly all, IFN-α production by pDC. These cells, which are found mainly in BM and spleen, ultimately differentiate into pDC that produce little or no IFN-α and instead promote immune tolerance. The latter cells, which also comprise a phenotypically distinct subset, are the main pDC in peripheral tissues. Thus, our data support a model in which immature pDC are proinflammatory, while mature, tissue-resident pDC are tolerogenic. Control of the frequency and tissue distribution of these functionally distinct pDC subsets provides an elegant mechanism by which IFN-α can be tightly regulated.

Material and methods

Mice and cell lines

Female or male C57BL/6 and Sv129 mice were obtained from Jackson Laboratories (Bar Harbor, ME) and used at 8–12 weeks of age. OT-I and OT-II OVA-TcR transgenic mice crossed onto Rag-1−/− background were purchased from Taconic Farms (Germantown, NY) and bred in-house. Congenic Ly5.1 (Ptprca) mice, Flt3L−/− and STAT-1−/− mice were obtained from Taconic. All experiments were performed under institutional guidelines according to approved protocols. The B16 melanoma cell line stably transfected with mouse Flt3L was a kind gift of Dr. G. Dranoff, Harvard University [13]. 3–4 million cells were injected subcutaneously and animals were sacrificed after 10–14 days. EG7 cells (EL4 thymoma transfected with OVA) were purchased from ATCC (Manassas, VA).

Cell preparation and flow cytometry

BM-derived DC were prepared by flushing the femur and tibia using a needle. DC derived from LN, thymus or liver were dispersed into single cell suspensions. Mouse blood was obtained by cardiac puncture, layered onto Ficoll-Hypaque and centrifuged for 20 min at 800×g. After washing, total leukocytes were stained with directly FITC-conjugated antibodies to CD3, CD19, DX5 and Ly6G (to exclude T cells, B cells, NK cells and granulocytes), CD11b-Pacific Blue, CD11c-APC-Cy7 (all from Biolegend, San Diego, CA) B220-Pacific Orange (Invitrogen, Carlsbad, CA) and CD9-Alexa Fluor 647 (Biolegend) and sorted using a FACSAria (Becton Dickinson, Mountain View, CA). Propidium iodide was included to gate out dead cells. Gates were set on forward and side scatter, lineage positive cells and myeloid DC were excluded, whereas CD11c+B220+ cells were sorted into $CD9^{pos}$ and $CD9^{neg}$ subsets. Purity of sorted cells typically exceeded 95% (Data not shown). Splenic pDC and total CD11c DC were isolated using CD11c-conjugated magnetic beads (Miltenyi Biotech) and then stained as above. OVA-specific CD4+ or CD8+ T cells were isolated from the spleens of OT-II-Rag−/− or OT-I-Rag−/− mice. Spleens were dispersed into a single cell suspension, anti-CD4 or anti-CD8 conjugated magnetic beads (Miltenyi) were added and cells were incubated for 20 min at 4°C after which they were separated using a MACS magnet. Purity was typically >90%. T cells were labeled with CFSE (1 μM) for 10 min at 37°C, washed, and resuspended in Hepes-buffered RPMI 1640 supplemented with 10% FCS, antibiotics and 2mM L-glutamine. A total of 1×10^5 DC and 2×10^5 T cells were cultured in 96-well round-bottomed plates at a final volume of 200 μL. Cultures were supplemented with OVA peptide. Fluorochrome labeled antibodies were obtained from eBioscience (CD4, CD8αα, CD40, CD80, CD86, CD135, CCR7) BD (ICOS-L, OX40-L, Ly-6C, IAb/d, H2-Kb, CD62L, CD74, CD103) R&D Systems (CCR6, CCR9), Invitrogen (B220 Pacific Orange), Serotec (CD200R) or Biolegend (CD3, CD11b, CD11c, CD19, DX-5, Siglec-H, CD38). G120.8 was obtained from Schering Plough Biopharma and conjugated with Alexa Fluor 488 (Inivtrogen) according to the manufacturer's instruction. PDCA-1 was purchased from Miltenyi Biotech.

Cytokine assays

Supernatants from DC were harvested after 24–48 hours of culture, and stored at −20°C until measured by ELISA. TLR agonists (CpG 2336, 1826 and 1585 (TLR9), gardiquimod, Pam_3CSK4 (synthetic triacylated lipoprotein, TLR1/2), FSL-1 (TLR2/6), R848 (TLR7/8)) were obtained from InvivoGen, San Diego, CA. Polyinocytidine (poly I:C, TLR3 agonist) and LPS (TLR4 agonist) were from Sigma. DC-T cell co-cultures were restimulated after 7 days using PMA and ionomycin (Sigma). Supernatants were analyzed by ELISA. Detection of intracellular IFN-α was performed as described [14]. Briefly, total BM derived cells were cultured for 9 hours with or without CpG 2336 motifs. Brefeldin A was added after 3 hours. Cells were fixed and permeabilized as described by the manufacturer (eBioscience), and a mixture of rat anti-mouse IFN-α antibodies RMMA (R&D Systems) and F18 (Abcam) was added. Cells were further incubated with rabbit anti-rat IgG Alexa Fluor 488 (Invitrogen) and total rat IgG (Sigma) was then used for blocking. Directly fluorochrome labeled antibodies to CD11c and B220 were added, and cells were analyzed by flow cytometry.

Electron microscopy

Transmission electron microscopy was performed using standard procedures [2]. Briefly, freshly FACS sorted DC were washed and fixed in 2.5% glutaraldehyde in cacodylate buffer and postfixed in 1% OsO4 solution. Cells were dehydrated in a series of alcohol solutions and embedded in epoxide. Sections were examined using a JEOL 1230 microscope (JEOL, Peabody, MA) at the Stanford Core Facility for biologic imaging.

PCR

pDC were FACS sorted as above and frozen in 10% DMSO, 50%FCS in PBS in liquid nitrogen. Cells were further washed in PBS and RNA was isolated using an RNeasy microkit (Qiagen, Valencia, CA, according to the manufacturer's instruction). cDNA was synthesized using Applied Biosystem's High Capacity Reverse Transcription kit (Foster City, CA) according to the manufacturer's instruction. PCR was performed using Taq DNA polymerase and buffer mix (Qiagen) in the presence of oligonucleotide primers for E2-2, IRF-7 and β-actin (control) genes. E2-2 primers: forward 5′-AGACCAAGCTCCTGATTCTC-3′; reverse 5′-AGGCTCTAGGACACCTTC-3′ (134 pb product). IRF-7 primers: forward 5′-CCTGTGTAGACGGAGCAATG-3′; reverse 5′-GTACAGGAACACGATCTGG-3′ (821 bp product). β-actin primers: forward 5′-TGGAATCCTGTGGCATCCATGAAAC-3′; reverse 5′-TAAAACGCAGCTCAGTAACAGTCCG-3′ (349 pb product). The cycling conditions were as follows: initial denaturation at 94°C for 3 min 45sec, followed by 35 cycles of 94°C for 45 sec, 55°C for 30 sec and 72°C for 1 min 30 sec and a final extension step at 72°C for 10 min. Amplified cDNA was run on 2% agarose gels, stained with propidium iodide and visualized using a UV-trans-illuminator.

CTL assay and tumor model

For detection of CTL activity, EG7 (OVA transfected) tumor cells were labeled with a high concentration of CFSE and control EL4 cells were labeled with a low CFSE concentration [15], mixed in equal parts, and used as target cells. Graded numbers of effector OT-I T cells, either unstimulated or cultured with the respective peptide-pulsed (SINFEKL, 100 ng/ml) pDC subsets for 3 days, were added to the labeled target cells. Specific lysis was determined by FACS according to the following formula: ratio = (percentage of $CFSE^{low}/CFSE^{high}$); percentage of specific lysis = (1-(ratio unprimed/ratio primed) x100).

Groups of mice were given peptide-pulsed ($OVA_{257–264}$, 100 ng/ml)) pDC subsets by subcutaneous injection in the footpad (0.5×10^6/mouse) at day -14 and day -7. On day 0,

mice were challenged by injection of 0.1×10^6 EG7 cells into the flank. Tumor growth was measured every other day. At the termination of the experiment, mice were sacrificed and tumor-draining LN and contralateral LN were harvested and analyzed for the presence of FoxP3+ CD4 T cells by flow cytometry.

In vivo pDC differentiation

Sorted pDC or pDC subsets were labeled with CFSE (Invitrogen), washed and injected intravenously into congenic CD45.1 recipient mice. 2–5 days after injection, various organs were harvested and assessed for the presence of CFSE+ pDC using multicolor flow cytometry. On day 4 after transfer, spleen and LN were harvested, pooled and CFSE+ pDC were isolated by sorting with a FACS Aria II. The sorted cells were cultured in the presence of CpG motifs, after which supernatants were harvested and stored at −20°C until assayed for IFN-α production by ELISA. pDC from Sv129 mice were sorted into subsets and injected intravenously into STAT-1 −/− mice, which are unable to secrete type I interferon [16]. Mice were given a simultaneous injection of CpG 2336 (100 μg/mouse). These recipients were chosen due to their inability to secrete type I interferon. Hence, only adoptively transferred cells are able to respond to TLR9 ligation. 6 hours after injection, serum was collected and frozen until analyzed for the presence of IFN-α.

Statistical analysis

Comparison of means was performed using paired or unpaired two-tailed Student's T-test (Graph Pad Prism). Tumor growth was evaluated by one-way ANOVA.

Results

$CD9^{pos}$ pDC, but not $CD9^{neg}$ pDC, produce IFN-α

Activation of pDC with oligodinucleotides containing CpG motifs leads to IFN-α production. However, as shown in Figure 1A, only a fraction of pDC produce this cytokine, suggesting that the IFN-α secreting cells may comprise a discrete pDC subset. In an effort to identify markers that might distinguish such a subset, we surveyed the expression of selected surface markers on BM derived pDC. Among these, CD9, a tetra-membrane spanning protein [17], appeared to define a clearly discernable subpopulation. To confirm this observation and study the functions of $CD9^{pos}$ and $CD9^{neg}$ pDC, we injected mice with an fms-like tyrosine kinase ligand (Flt3-L) secreting tumor cell line that increases the yield of pDC [13]. 10–14 days later, we stained BM cells with antibodies to CD11c, B220 and CD9. myDC and lineage positive cells were excluded (Supplementary Fig. 1). pDC were defined as co-expressing CD11c and B220 [2, 3], and were further subdivided into CD9 negative ($CD9^{neg}$) and CD9 positive ($CD9^{pos}$) fractions.

To assess the function of these cells, sorted $CD9^{pos}$ and $CD9^{neg}$ pDC were cultured with various Toll-like receptor (TLR) agonists for 48 hours, before measuring IFN-α and other cytokines in the supernatants. As shown in Figure 1B, the $CD9^{pos}$ pDC are the major IFN-α producing cells, and only small amounts of IFN-α could be detected in the cultures of CpG-stimulated $CD9^{neg}$ pDC. Since different CpG motifs may induce different levels of IFN-α, we cultured our pDC subsets in the presence of CpG 2336 and 1585 (both CpG-A type) and 1826 (CpG-B) for 48 hours and analyzed the supernatants for IFN-α. Only the $CD9^{pos}$ pDC produced IFN-α in response to CpG-A, whereas neither subset produced IFN-α in response to CpG-B (Figure 1B). In fact, $CD9^{neg}$ pDC did not produce IFN-α above background levels, regardless of the source of CpG (Figure 1B). It is possible that $CD9^{neg}$ pDC lack the synthetic machinery proximal signaling components or TLR receptors needed to respond to exogenous stimuli and produce IFN-α. It is also possible that these cells are not pDC at all, but simply share a similar surface phenotype with pDC. To help address this question, we

determined the expression of E2-2, a pDC-specific transcription factor [18], in $CD9^{pos}$ and $CD9^{neg}$ pDC. Both subsets expressed equal amounts of E2-2 irrespective of IFN-α secretion as detected by reverse transcriptase PCR (RT-PCR) (Figure 1C). Likewise, interferon regulatory factor 7 (IRF7), the main transcription factor responsible for IFN-α expression in pDC [19], was present in both subsets (Figure 1C). The level of expression of these two transcription factors remained unchanged after stimulation with CpG. As CpG motifs signal through TLR9, we examined the expression of this receptor by intracellular staining. Figure 1D shows that the two subsets express similar levels of TLR9.

Mouse pDC can produce other cytokines, mainly IL-6, TNF-α, and IL-12, in contrast to human pDC, which do not produce IL-12 [20]. Furthermore, and unlike human pDC, mouse pDC express all TLRs [21]. On this basis, we examined the cytokine response to the different TLRs (Supplementary Figure 2A). IL-6, TNF-α and IL-12 were all produced by the $CD9^{pos}$ cells, whereas the $CD9^{neg}$ cells produced TNF-α but little IL-6 or IL-12. To validate these *in vitro* data, we examined the capacity of $CD9^{pos}$ and $CD9^{neg}$ pDC to produce IFN-α *in vivo*. Sorted pDC derived from Sv129 mice, in combination with CpG 2336, were injected into signal transducers and activation of transcription-1 (STAT-1) deficient recipients (Sv129 background), which are unable to produce IFN-α in response to CpG motifs. Sera were collected and analyzed for IFN-α by ELISA. Only mice that received $CD9^{pos}$ pDC showed detectable serum levels of IFN-α (Supplementary Figure 2B).

CD9 identifies a subset of pDC with a distinct surface phenotype

DCs isolated from mice injected with an Flt3-L secreting tumor cell line were harvested from BM. As shown in Figure 2A, $CD9^{neg}$ and $CD9^{pos}$ pDC differ in their expression of many surface antigens. The $CD9^{neg}$ cells express high levels of the inflammatory chemokine receptor CXCR3, the pDC antigens Siglec-H and PDCA-1, CD4 and CD8αα. $CD9^{pos}$ pDC express low levels of Siglec-H and PDCA-1, and little CD4 and CD8αα, but intermediate levels of MHC class II, CD86, inducible costimulator (ICOS)-L, and the gut homing receptor α4β7, and high levels of CD62L and OX40-L (Figure 2A). A more complete phenotype of each subset is shown in Supplementary Figure 3. CCR9 was recently reported to be expressed on tolerogenic pDC [22]. Not surprisingly, this molecule is highly expressed on $CD9^{neg}$ pDC and absent from the surface of $CD9^{pos}$ pDC (Figure 2A). Interestingly, however, when the $CD9^{pos}$ subset was cultured overnight in medium alone, CCR9 appeared rapidly on the cell surface, suggesting that this molecule may have been pre-formed in these cells (Supplementary Fig. 4 upper panel). Intracellular staining of freshly isolated $CD9^{pos}$ cells for CCR9 confirmed this notion (Supplementary Figure 5).

Morphological differences between pDC subsets

The designation “plasmacytoid” refers to the similar appearance of pDC and plasma cells when examined using electron microscopy (EM), with both cell types showing well-developed RER [1]. Given the dramatic differences in the capacity of $CD9^{pos}$ and $CD9^{neg}$ subsets to produce IFN-α, we wanted to determine whether these cells also differed when examined by EM. Figure 2B show that whereas the BM-derived $CD9^{pos}$ pDC contain abundant rough endoplasmic reticulum (RER) and have a very electron dense cytoplasm, the $CD9^{neg}$ DC have little RER, larger nuclei and many vacuoles. Thus, the ultrastructure of the $CD9^{neg}$ pDC does not correspond to that of a classical IFN-α secreting pDC.

We further analyzed the relative frequencies of the $CD9^{pos}$ and $CD9^{neg}$ pDC subsets in different tissues of Flt3-L treated mice. Although pDC could be obtained in greater numbers from BM and spleen, they were also present in peripheral lymph nodes (LN) and liver, as reported previously [2, 3, 23]. Interestingly, in the thymus and mediastinal LN, the $CD9^{neg}$ subset predominated (Figure 3A). Mediastinal pDC have been reported to induce tolerance

to airborne antigens [24], and FACS analysis showed that these cells were almost exclusively of the $CD9^{neg}$ subtype, while expressing high levels of the Siglec-H, PDCA-1 and the chemokine receptor CCR9 (an early response gene for pDC [18]) (Figure 3B). We therefore stimulated pDC from thymus and mediastinal LN and assessed their capacity to secrete IFN-α. The results show that pDC from these tissues produce very small amounts of IFN-α compared to BM-derived pDC (Figure 3C). Moreover, when isolating total pDC (CD11c+B220+) versus myeloid DC (CD11c+CD11b+) from BM, spleen or LNs of Flt-3L treated mice, pDC from BM secreted at least twice as much IFN-α compared with pDC from spleen or LNs (Supplementary Figure 6).

$CD9^{pos}$ and $CD9^{neg}$ pDC induce the production of different cytokines from CD4+T cells in vitro

We further examined the T cell stimulatory capacity of the two pDC subsets. To this end, carboxy-fluorescein succimide ester (CFSE)-labeled CD4+ OT-II T cells were cultured together with an immunodominant ovalbumin (OVA) peptide ($OVA_{323–339}$) and $CD9^{pos}$ or $CD9^{neg}$ pDC for 6–7 days. Cells were restimulated using phorbol myristate acetate (PMA) and ionomycin, and the T cell culture supernantant was harvested and analyzed by ELISA for cytokine secretion. Whereas the antigen-pulsed $CD9^{pos}$ pDC induced vigorous CD4+ T cell proliferation, T cells cultured with $CD9^{neg}$ pDC underwent few divisions (Figure 4A). Moreover, CD4+ T cells cultured with $CD9^{pos}$ pDC produced IFN-γ but little or no IL-4 and IL-10, whereas the T cells cultured with the $CD9^{neg}$ subset produced mainly IL-4 and IL-10 (Figure 4B). In addition, $CD9^{neg}$ pDC could induce the production of TGF-β, a cytokine typically associated with regulatory T cells (Figure 4C).

$CD9^{pos}$ pDC promote CD8+ T cell activation and CTL formation

We proceeded to examine the response of CD8+ T cells to $CD9^{pos}$ and $CD9^{neg}$ pDC, as such T cells are an important component of anti-viral and anti-tumor immunity and are known to be activated by IFN-α producing cells [1, 4]. We pulsed each pDC subset with the immunodominant OVA peptide SINFEKL ($OVA_{257–264}$) and cultured these pDC with CD8+ OT-I T cells. $CD9^{pos}$ pDC induced a strong CD8+ T cell response, whereas the $CD9^{neg}$ subset induced little proliferation (Figure 4D). To assess whether $CD9^{pos}$ pDC could induce functional CTL as determined by lysis of EG7 tumor cells, we cultured each pDC subset together with OT-I T cells for 4 days. After washing, the T cells were incubated with CFSE-labeled EL-4 and EG7 tumor cells to analyze their cytotoxic capacity. As shown in Figure 4E, $CD9^{pos}$ pDC alone induced CTL capable of causing EG7 cell lysis in a dose-dependent manner.

To test the activity of $CD9^{pos}$ and $CD9^{neg}$ pDC in a tumor model, we injected $OVA_{257–264}$ -pulsed $CD9^{pos}$ or $CD9^{neg}$ pDC (0.5×10^6 cells/animal) into the footpads of groups of tumor-naïve, syngenic mice. Control animals were given phosphate buffer saline. One week after the first injection, the mice were given a second injection of similarly prepared pDC. One week after the second injection, mice were challenged with EG7 tumor cells (0.1×10^6/animal) subcutaneously in the flank. Tumor growth was monitored every two days. As shown in Figure 5A, injection of $CD9^{pos}$ pDC completely prevented tumor growth whereas $CD9^{neg}$ pDC had little or no anti-tumor effect such that tumors in these mice grew to the same extent seen in the saline control group. When examining the LN of treated mice, we found that mice that received $CD9^{neg}$ pDC had increased numbers of FoxP3+ CD4+ T cells in their tumor-draining LN compared with the contralateral LN (Figure 5B). Vα2TcR +FoxP3+ CD4+ T cells were also present (Figure 5B, lower panel). A similar increase could not be found in the draining LN of the control group or in mice given $CD9^{pos}$ pDC.

CD9 expression is gradually lost on pDC in vivo

To assess the stability of CD9 expression on pDC *in vivo*, total BM-derived pDC or purified $CD9^{pos}$ pDC ($2–5\times10^6$ cells) from Flt-3L-treated mice were labeled with CFSE and injected intravenously into congenic CD45.1 mice. After 2–4 days, various organs were harvested and examined for CD9 expression using flow cytometry (Figure 6A). As shown in Figure 6B, most $CD9^{pos}$ cells had become $CD9^{neg}$ *in vivo* and upregulated Siglec-H. To determine whether pDC that matured *in vivo* lose their ability to secrete IFN-α, we transferred CFSE-labeled $CD9^{pos}$ pDC into congenic recipients. Four days after transfer, spleen and LN were harvested, and pooled into a single cell suspension. Cells were sorted based on their expression of CFSE and CD45.2, excluding lineage positive and CD45.1 cells. As shown in Figure 6C, the transferred pDC secreted less IFN-α compared with pDC freshly isolated from BM.

Flt3-L promotes pDC viability

As Flt3-L is a crucial growth factor for pDC development and differentiation *in vitro* and *in vivo* [25–27], we asked whether addition of Flt3-L to the respective subsets would affect their differentiation *in vitro*. To this end, sorted $CD9^{pos}$ and $CD9^{neg}$ pDC were cultured in the presence or absence of Flt3-L (100 ng/ml) and/or CpG 2336 motifs (10 μg/ml) for 4 days, and viability and phenotypic changes were assessed daily. As shown in Figure 7A, pDC cultured in medium alone rapidly lost their viability and after 3 days all the cells were dead. By contrast, pDC culture in Flt3-L survived longer and half of the cells were still viable after 3 days of culture. The $CD9^{pos}$ cells remained viable longer than their $CD9^{neg}$ counterparts. Activation of $CD9^{pos}$ pDC with CpG motifs in the presence of FL resulted in reduced survival. Moreover, whereas the phenotype of the $CD9^{neg}$ pDC appeared stable in medium or Flt3-L, the $CD9^{pos}$ cells gradually lost expression of CD9, and upregulated that of Siglec-H, PDCA-1 and CCR9, indicative of differentiation into $CD9^{neg}$ pDC (Figure 7B). In the presence of CpG 2336, CD9 expression was rapidly downregulated on $CD9^{pos}$ pDC, and Siglec-H was not induced (Supplementary Figure 4). However, stimulation with CpG 2336 had little effect on the $CD9^{neg}$ pDC.

To assess the effect of Flt3-L on pDC subset differentiation *in vivo*, we transferred sorted pDC subsets (CD45.1) into Flt3-L KO recipients (CD45.2). 2–4 days later, we harvested the spleens of the Flt3-L KO mice and examined the expression of CD9 and Siglec-H on the transferred pDCs. Figure 7C shows, that $CD9^{pos}$ pDC differentiate into $CD9^{neg}$ cells even in the absence of Flt3-L, although not to the same extent as in wt C57BL/6 recipients (Figure 7B).

Discussion

We initiated this study with the objective of understanding how a single cell type can mediate both proinflammatory [1–4] and suppressive [5–8] immune responses, and how these activities relate to the most critical function of pDC, namely the production of IFN-α [1–4, 28]. Our data show that the opposing functions of pDC are not mediated by a single phenotypically stable cell type, but by distinct subsets that differ in surface phenotype, morphology and function. Furthermore, the results indicate that these subsets represent pDC in different stages of maturation: an early stage cell with the capacity to produce IFN-α and other proinflammatory mediators, and a later stage cell that can no longer produce these factors but is instead tolerogenic. Thus, the two pDC subsets do not originate from different precursor populations, but rather from a single precursor undergoing a natural differentiation process. Flt3-L plays an important part in promoting viability of the pDC during this differentiation process (Figure 7A) [26, 27]. However, the transition into $CD9^{neg}$ Siglec-H^{high} pDC can proceed in the absence of exogenous Flt3-L, suggesting that other factors

may promote pDC differentiation. The data also support a model in which immature pDC are proinflammatory, whereas mature pDC are regulatory or suppressive.

We considered the possibility that one or both of our DC populations studied here might contain myeloid DC, in light of a recent publication suggesting that some CD11c+B220+ cells are precursors of conventional myeloid DC [29]. However, the CD11c+B220+ cDC precursors are PDCA1 (CD317) and Siglec-H negative and produce little IFN-α, whereas the CD9+CD11c+B220+ subset identified in our study is PDCA1+ and produces large amounts of IFN-α. Moreover, our Siglec-H^{pos} CD9^{neg} cells produce little IFN-α but express more PDCA-1 than CD9+ pDC. These data argue strongly that few, if any, of the CD9+ cells studied here are cDC.

Since IFN-α is a potent cytokine with direct effects on many other cell types, such as NK cells and B cells, it is important that the production of IFN-α be tightly regulated. Our data show, that under steady-state conditions only immature CD9^{pos} pDC, which are found mainly in the BM and spleen, can produce IFN-α and other inflammatory cytokines. In contrast, pDC found in tissues such as thymus, liver and the LN draining the lung and gut, are mostly CD9^{neg} pDC and no longer produce inflammatory cytokines. Indeed, these cells appear to be tolerogenic. A schematic representation of these findings is shown in Supplementary Figure 7.

The mechanism responsible for the inability of CD9^{neg} pDC to produce substantial quantities of IFN-α is unknown. These cells, like CD9^{pos} cells, express at least some of the synthetic machinery required for IFN-α production, including IRF7, the main IFN-α transcription factor [19] (Figure 1C). They also express TLR9 at levels similar to that seen in CD9^{pos} cells. Further, there is no question of their identity as pDCs since they express the pDC defining transcription factor E2-2 [18] as well as the pDC specific molecule, Siglec-H [30]. Indeed, Siglec-H, which mediates signals via DAP-12 that inhibit IFN-α production, is expressed at higher levels on CD9^{neg} than CD9^{pos} cells, and exposure of CD9^{pos} pDC to CpG motifs results in upregulation of MHC class II and CD86, but not of Siglec-H (Supplementary Figure 4), thus providing a feedback mechanism by which IFN-α production can be maintained [31]. Regardless of the molecular basis for the differences in IFN-α production between CD9^{pos} and CD9^{neg} pDC, the sequestering of the most potent IFN-α producing cells away from peripheral tissues, during the steady-state, may provide a mechanism that helps avoid the development of autoimmune disease. On the other hand, activation of CD9^{pos} pDC during infection may not only induce their secretion of IFN-α, but may also induce their migration to LN and/or sites of infection.

In a recent report [22] mouse pDC were divided into functionally distinct subsets based on their expression of CCR9, which correlated with the capacity to home to the small intestine [32]. Our results show that the CCR9+ pDC are contained in, and correspond to, the CD9^{neg} pDC. Interestingly, we find abundant CCR9 in the cytoplasm of CD9^{pos} pDC, which would explain the rapid appearance of this molecule on the surface of cultured or injected CD9^{pos}CCR9- pDC. Although experiments described in the earlier report suggested that CCR9+ and CCR9- pDC were equally capable of producing IFN-α, the CpG oligonucleotide (1826) used in that study to activate pDC is not a strong inducer of IFN-α production (Figure 1C) and, therefore, probably would not have revealed the differences we observed.

Several other surface antigens that were differentially expressed on the pDC subsets may contribute to their functional differences. CD9, a co-receptor for MHC class II on DC [17], likely plays a role in the enhanced T cell stimulation by the CD9^{pos} pDC. PDCA-1 and G120.8, two pDC related molecules recognizing the bone marrow stromal cell antigen (BST)-2 [33] are also upregulated upon pDC maturation. The function of BST-2 is at the

present time unknown, although it has been postulated to participate in the down-regulation of IFN-α secretion [33]. ICOS-L and OX40-L, both T cell co-stimulatory molecules, are higher on the $CD9^{pos}$ pDC population, and are likely to contribute to the superior ability of this subset to activate T effector cells. On the other hand, expression of CD4 and CD8αα, is highest on $CD9^{neg}$ pDC and does not appear to correlate with T cell stimulatory capacity, as reported for myeloid DC [34]. α4β7 and CD62L, molecules involved in homing to the small intestine and to peripheral LNs, respectively, are highly expressed on the $CD9^{pos}$ pDC.

Our data show that $CD9^{pos}$ pDC can induce potent anti-tumor immunity. Conversely, the CCR9+ pDC [22], which correspond to the $CD9^{neg}$ subset, can protect against graft versus host disease, which is consistent with our finding that $CD9^{neg}$ pDC induce FoxP3+ T reg cells in our tumor model. As recently shown [35], ablation of all DC *in vivo* in the steady-state leads to uncontrolled autoimmunity. Although we do not have any evidence at present that the pDC subsets described here contribute to disease pathogenesis, it is tempting to speculate that the $CD9^{pos}$ pDC may participate in the development of autoimmune diseases (eg., SLE, psoriasis and diabetes [10–12]) in which IFN-α has been implicated. Conversely, accumulation of mature $CD9^{neg}$ pDC in tumors may have negative clinical consequences, as our data suggest that these cells induce the formation of FoxP3+ Treg cells in tumor draining LN. A number of published studies indicate that tumor prognosis is inversely related to the number of tumor-infiltrating pDC and Treg cells [36–38]. Thus, despite the fact that $CD9^{pos}$ pDC can induce strong anti-tumor immunity, using these cells, or pDC TLR agonists, for the treatment of cancer presents a risk that their maturation into tolerogenic cells may contribute to tumor growth.

Supplementary Material

Refer to Web version on PubMed Central for supplementary material.

Acknowledgments

We thank Drs. R.G. Morris and R. de Waal Malefyt for helpful comments on the manuscript, and Drs T. Iwahori, K. Heydari and Mrs. L. Tolentino for FACS sorting.

References

1. Liu YJ. IPC: Professional type I interferon-producing cells and plasmacytoid dendritic cell precursors. Ann Rev Immunol. 2005; 23:275–306. [PubMed: 15771572]
2. Björck P. Isolation and characterization of plasmacytoid dendritic cells from Flt3 ligand and granulocyte-macrophage colony-stimulating factor-treated mice. Blood. 2001; 98:3520–3526. [PubMed: 11739152]
3. Asselin-Paturel C, Boonstra A, Dalod M, Durand I, Yessaad N, Dezutter-Dambuyant C, Vicari A, O'Garra A, Briere F, Trinchieri G. Mouse type I IFN-producing cells are immature APCs with plasmacytoid morphology. Nat Immunol. 2001; 2:1144–1150. [PubMed: 11713464]
4. Colonna M, Trinchieri G, Liu Y-J. Plasmacytoid dendritic cells in immunity. Nat Immunol. 2004; 5:1219–1226. [PubMed: 15549123]
5. Ochando JC, Homma C, Yang Y, Hildago A, Garin A, Taccke F, Angeli V, Li Y, Boros P, Ding Y, Jessberger R, Trinchieri G, Lira SA, Randolph G, Bromberg JS. Alloantigen-presenting plasmacytoid dendritic cells mediate tolerance to vascularized grafts. Nat Immunol. 2006; 7:652–662. [PubMed: 16633346]
6. Björck P, Coates PT, Wang Z, Duncan FJ, Thomson AW. Promotion of long-term heart allograft survival by combination of mobilized plasmacytoid dendritic cells and anti-CD154-monoclonal antibody. J Heat Lung Transplant. 2005; 24:118–1120.

7. Goubier A, Dubois B, Gheit H, Joubert G, Villard-Truc F, Asselin-Paturel C, Trinchieri G, Kaiserlian D. Plasmacytoid dendritic cells mediate oral tolerance. Immunity. 2008; 29:1–12. [PubMed: 18631448]
8. Steinman RM, Hawiger D, Nussenzweig MC. Tolerogenic dendritic cells. Ann Rev Immunol. 2003; 21:685–711. [PubMed: 12615891]
9. Curotto de Lafaille MA, Lafaille JJ. Natural and adaptive FoxP3+ regulatory T cells: more of the same or division of labor? Immunity. 2009; 30:626–635. [PubMed: 19464985]
10. Vollmer J, Tluk S, Schmidt C, Hamm S, Jurk M, Forsbach A, Akira S, Kelly KM, Reeves WH, Bauer S, Krieg AM. Immune stimulation mediated by autoantigen binding sites within small nuclear RNAs involves Toll-like receptors 7 and 8. J Exp Med. 2005; 202:1575–1585. [PubMed: 16330816]
11. Nestle FO, Conrad C, Tun-Kui A, Homey B, Gombert M, Boyman O, Burg G, Liu Y-J, Gilliet M. Plasmacytoid pre-dendritic cells initiate psoriasis through interferon-α production. J Exp Med. 2005; 202:135–143. [PubMed: 15998792]
12. Li Q, Xu B, Michie SA, Rubins KH, Schreiber RD, McDevitt HO. Interferon-α initiates type 1 diabetes in nonobese diabetic mice. PNAS. 2008; 105:12439–12444. [PubMed: 18716002]
13. Mach N, Gillessen S, Wilson SB, Sheehan C, Mihm M, Dranoff G. Differences in dendritic cells stimulated in vivo by tumors engineered to secrete granulocyte-macrophage colony-stimulating factor or Flt3-ligand. Cancer Res. 2000; 60:3239–3246. [PubMed: 10866317]
14. Asselin-Paturel C, Brizard G, Chemin K, Boonstra A, O'Garra A, Vicari A, Trinchieri G. Type I interferon dependence of plasmacytoid dendritic cell activation and migration. J Exp Med. 2005; 201:1157–1167. [PubMed: 15795237]
15. Curtsinger JM, Lins DC, Mescher MF. Signal 3 determines tolerance versus full activation of naïve CD8 T cells: dissociating proliferation and development of effector function. J Exp Med. 2003; 197:1141–1151. [PubMed: 12732656]
16. Meraz MA, White JM, Sheehan KC, Bach EA, Rodig SJ, Dighe AS, Kaplan DH, Riley JK, Greenlund AC, Campbell D, Carver-Moore K, DuBois RN, Clark R, Aguet M, Schreiber RD. Targeted disruption of the Stat1 gene in mice reveals unexpected physiologic specificity in the JAK-STAT signaling pathway. Cell. 1996; 84:431–442. [PubMed: 8608597]
17. Unternaehrer JJ, Chow A, Pypaert M, Inaba K, Mellman I. The tetraspanin CD9 mediates lateral association of MHC class II molecules on the dendritic cell surface. PNAS. 2007; 104:234–239. [PubMed: 17190803]
18. Cisse B, Caton ML, Lehner M, Maeda T, Scheu S, Locksley R, Holmberg D, Zweier C, den Hollander NS, Kant SG, Holter W, Rauch A, Zhuang Y, Reizis B. Transcription factor E2-2 is an essential and specific regulator of plasmacytoid dendritic cell development. Cell. 2008; 135:37–48. [PubMed: 18854153]
19. Honda K, Ohba Y, Yanai H, Negishi H, Mizutani T, Takaoka A, Taya C, Taniguchi T. IRF-7 is the master regulator of type-I interferon-dependent immune responses. Nature. 2005; 434:772–777. [PubMed: 15800576]
20. Rissoan M-C, Soumelis V, Kadowaki N, Grouard G, Briere F, de Waal Malefyt R, Liu Y-J. Reciprocal control of T helper cell and dendritic cell differentiation. Science. 1999; 283:1183–1186. [PubMed: 10024247]
21. Edwards AD, Diebold SS, Slack EMC, Tomizawa H, Hemmi H, Kaisho T, Akira S, Reis e Sousa C. Toll-like receptor expression in murine DC subsets: lack of TLR7 expression by CD8α+ DC correlates with unresponsiveness to imidoazoquinolines. Eur J Immunol. 2003; 33:827–833. [PubMed: 12672047]
22. Haideba H, Sato T, Habtezion A, Oderup C, Pan J, Butcher EC. CCR9 expression defines tolerogenic plasmacytoid dendritic cells able to suppress acute graft-versus-host disease. Nat Immunol. 2008; 9:1253–1260. [PubMed: 18836452]
23. Lian ZX, Okada T, He XS, Kita H, Liu YJ, Ansari AA, Kikuchi K, Ikehara S, Gershwin ME. Heterogeneity of dendritic cells in the mouse liver: identification and characterization of four distinct populations. J Immunol. 2003; 170:2323–2330. [PubMed: 12594254]

24. de Heer HJ, Hammad H, Soullie T, Hijdra D, Vos N, Willart MA, Hoogsteden HC, Lambrecht BN. Essential role of lung plasmacytoid dendritic cells in preventing asthmatic reactions to harmless inhaled antigen. J Exp Med. 2004; 200:89–98. [PubMed: 15238608]
25. Gilliet M, Boonstra A, Paturel C, Antonenko S, Xu XL, Trinchieri G, O'Garra A, Liu YJ. The development of murine plasmacytoid dendritic cell precursors is differentially regulated by FLT3-ligand and granulocyte/macrophage colony-stimulating factor. J Exp Med. 2002; 195:953–958. [PubMed: 11927638]
26. Waskow C, Liu K, Darrasse-Jeze G, Guermonprez P, Ginhoux F, Merad M, Shenglia T, Yao K, Nussenzweig M. The receptor tyrosine kinase Flt3 is required for dendritic cell development in peripheral lymphoid tissues. Nat Immunol. 2008; 9:676–683. [PubMed: 18469816]
27. Liu K, Victora GD, Schwickert TA, Guermonprez P, Meredith MM, Yao K, Chu FF, Randolph GJ, Rudensky AY, Nussenzweig M. In vivo analysis of dendritic cell development and homeostasis. Science. 2009; 324:392–397. [PubMed: 19286519]
28. Gilliet M, Cao W, Liu Y-J. Plasmacytoid dendritic cells: sensing nucleic acids in viral infection and autoimmune diseases. Nat Immunol Rev. 2008; 8:594–606.
29. Segura E, Wong J, Villadangos JA. B220 CCR9 dendritic cells are not plasmacytoid dendritic cells but are precursors of conventional dendritic cells. J Immunol. 2009; 183:1514–1517. [PubMed: 19570827]
30. Blasius AL, Cella M, Maldonado J, Takai T, Colonna M. Siglec-H is an IPC-specific receptor that modulates type I IFN secretion through DAP12. Blood. 2006; 107:2474–2476. [PubMed: 16293595]
31. Blasius AL, Colonna M. Sampling and signaling in plasmacytoid dendritic cells: the potential roles of Siglec-H. TRENDS Immunol. 2006; 27:255–260. [PubMed: 16679063]
32. Wendland M, Czeloth N, Mach N, Malissen B, Kremmer E, Pabst O. CCR9 is a homing receptor for plasmacytoid dendritic cells to the small intestine. PNAS. 2007; 104:6347–6352. [PubMed: 17404233]
33. Blasius AL, Giurisato E, Cella M, Schreiber RD, Shaw AS, Colonna M. Bone marrow stromal cell antigen 2 is a specific marker of type I IFN-producing cells in the naïve mouse, but is a promiscuous cell surface antigen following IFN stimulation. J Immunol. 2006; 177:3260–3265. [PubMed: 16920966]
34. Shortman K, Liu Y-J. Mouse and human dendritic cell subtypes. Nat Rev Immunol. 2002; 2:151–161. [PubMed: 11913066]
35. Ohnmacht C, Pullner A, King SB, Drexler I, Meier S, Brocker T, Voehringer D. Constitutive ablation of dendritic cell breaks self-tolerance of CD4 T cells and results in spontaneous fatal autoimmunity. J Exp Med. 2009; 206:549–559. [PubMed: 19237601]
36. Zou W. Regulatory T cells, tumor immunity and immunotherapy. Nat Rev Immunol. 2006; 6:295–307. [PubMed: 16557261]
37. Zou W, Machelon V, Coulomb-L'Hermin A, Borvak J, Nome F, Isaeva T, Wei S, Krzysiek R, Durand-Gasselin I, Gordon A, Pustilnik T, Curiel DT, Galanaud P, Capron F, Emile D, Curiel TJ. Stromal-derived factor-1 in human tumors recruits and alters the function of plasmacytoid precursor dendritic cells. Nat Immunol. 2001; 7:1339–1346.
38. Treilleux I, Blay JY, Bendriss-Vermare N, Ray-Coquard I, Bachelot T, Guastalla JP, Bremond A, Goddard S, Pin JJ, Barthelemy-Dubois C, Lebeque S. Dendritic cell infiltration and prognosis of early stage breast cancer. Clin Cancer Res. 2004; 15:7466–7474. [PubMed: 15569976]

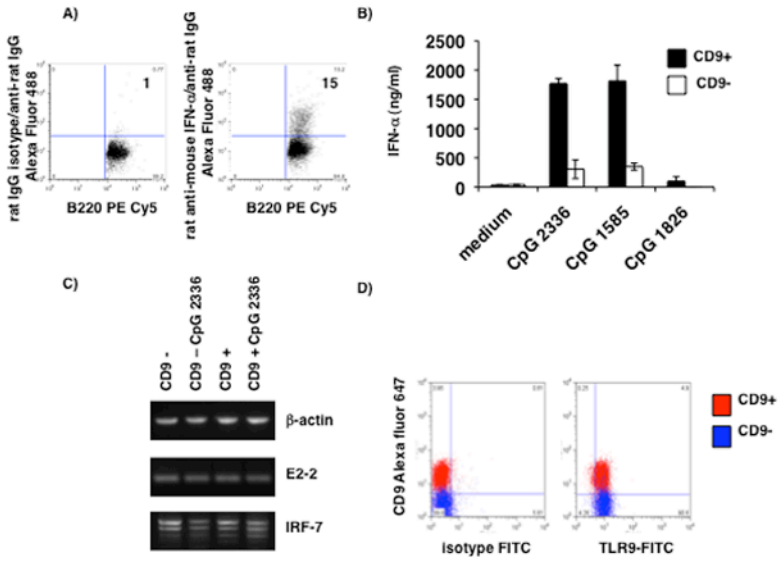

Figure 1. A phenotypically distinct subset of pDC produces IFN-α

(A) Only a fraction of BM- derived pDC produce IFN-α after stimulation with CpG 2336. Cells were gated on size and expression of CD11c and B220. (B) Sorted, CpG stimulated $CD9^{pos}$ pDC produce more IFN-α by comparison to identically stimulated $CD9^{neg}$ pDC (Student's paired T-test, CpG 2336 P=0.0472, CpG 1585 P=0.0210, CpG 1826, P=0.2074). $CD9^{neg}$ pDC do not produce IFN-α above background levels (CpG 2336 P=0.059, CpG 1585 P=0.132, CpG 1826 P=0.344) (s.d). (C) Both $CD9^{pos}$ and $CD9^{neg}$ pDC express the pDC-specific transcription factor E2-2, whether freshly isolated or after stimulation with CpG 2336. Both pDC subsets also express similar levels of IRF-7. (D) Both pDC subsets express similar levels of the CpG receptor TLR9 as determined by intracellular staining. The results shown are representative of 3 independent experiments.

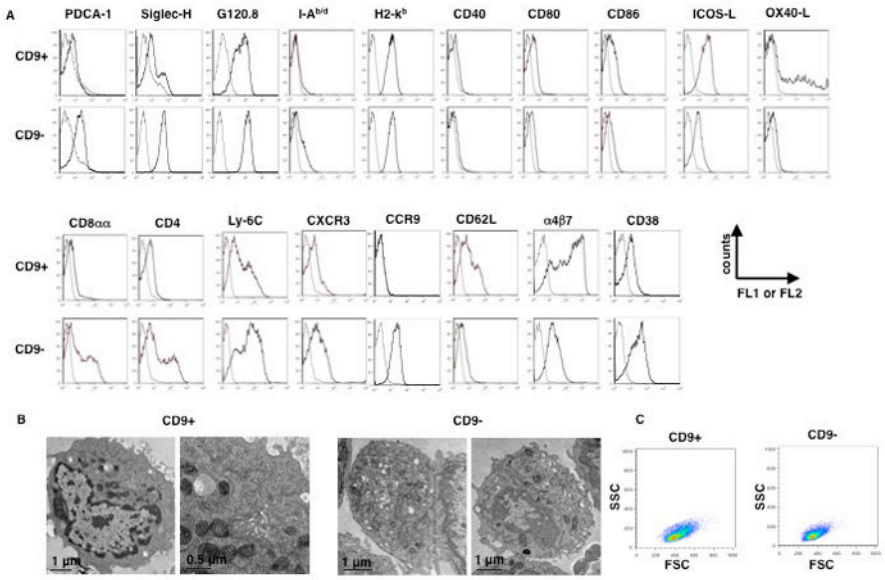

Figure 2. Many cell surface antigens are differentially expressed by the two pDC subsets

(A) FACS analysis of freshly sorted CD9^{pos} and CD9^{neg} subsets reveal differences in expression of the pDC selective antigens Siglec-H, PDCA-1 and G120.8. Additional surface antigens were also examined, as seen in Supplementary Figure 3. The results shown are representative of 5 independent experiments. (B) CD9^{pos} pDC contain abundant RER. CD9^{neg} pDC contain many vacuoles and lysosomes. (C) Size of CD9^{pos} and CD9^{neg} pDC based on forward and side scatter.

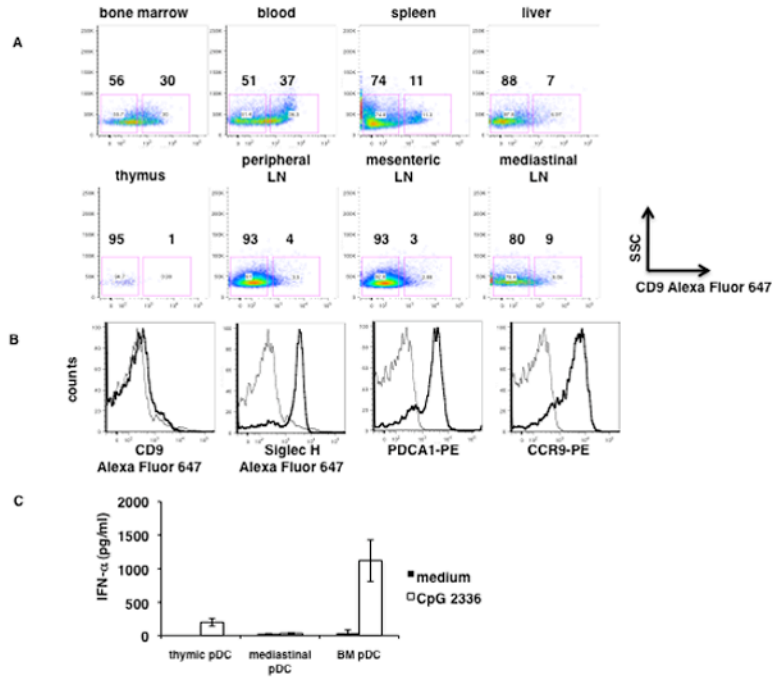

Figure 3. CD9^{pos} pDC are mainly found in the bone marrow

(A) Examination of different tissues reveals that BM and blood are the main sources of CD9^{pos} pDC whereas LN, thymus and liver contain mostly CD9^{neg} pDC. (B) Sorted pDC from mediastinal LN are mostly of the CD9^{neg} subset and express high levels of pDC-specific surface antigens. (C) Total pDC isolated from BM, thymus and mediastinal LN show that CpG-stimulated BM-derived pDC produce significantly more IFN-α than pDC obtained from thymus (Student's T test, P=0.004) or mediastinal LN (Student's T test, P=0.001). (s.d). The results shown are representative of 3 independent experiments.

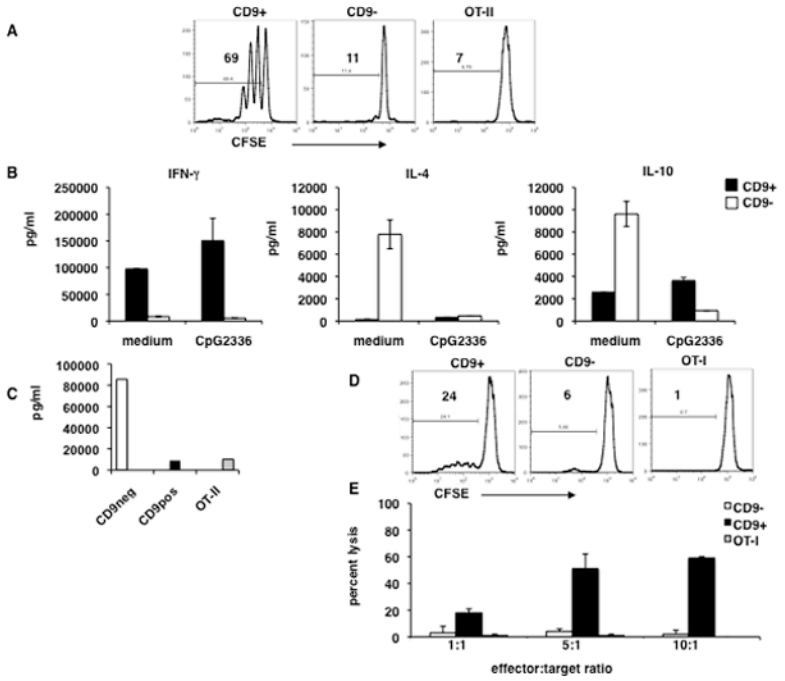

Figure 4. pDC subsets display different T cell co-stimulatory capacity

(A) Sorted pDC subsets (1×10^5) were pulsed with OVA323-339 (2 μg/ml) and cultured with CFSE-labeled OT-II T cells (2×10^5) for 4 days and T cell proliferation was measured by flow cytometry. (B) Sorted pDC subsets (1×10^5) pulsed with OVA323-339 (2 μg/ml) were stimulated over night, alone or in the presence of CpG 2336 (10 μg/ml). OT-II T cells were added and the cells were further cultured for 7 days. Cultures were stimulated with PMA and ionomycin for 24 hours, after which the cell supernatants were harvested and analyzed by ELISA. (s.d). (C) Sorted pDC subsets were cultured together with OT-II T cells in medium alone, and TGF-β was analyzed by ELISA. (D) Sorted pDC subsets (1×10^5) pulsed with OVA257-264 (100 ng/ml) were cultured with CFSE-labeled OT-I T cells (2×10^5) for 4 days and T cell proliferation was measured by flow cytometry. (E) pDC subsets were cultured with OT-I T cells for 4–5 days as above. T cells were washed, and further cultured together with OVA-expressing tumor target cells (EG7) labeled with a high concentration of CSFE. Non-OVA expressing EL4 tumor cells labeled with a low concentration of CFSE were used as an internal control. CTL activity was measured as percent lysis of EG7 cells. (s.d). The results are representative of 5 independent experiments.

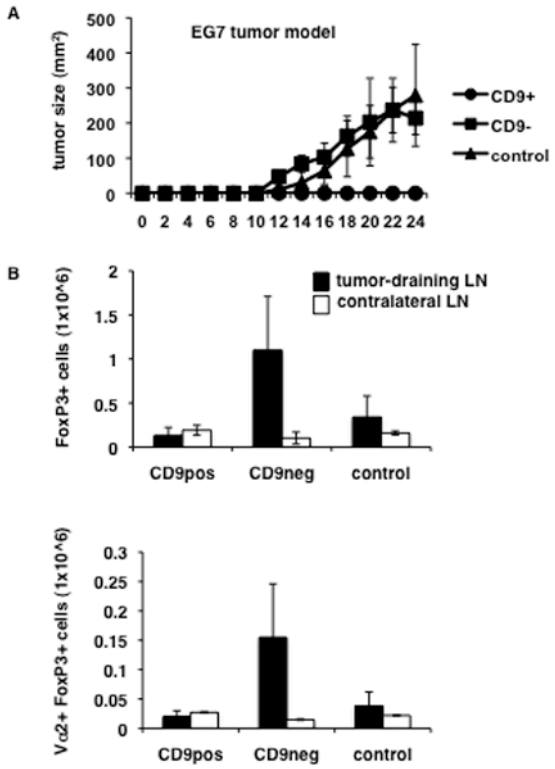

Figure 5. CD9^{pos} pDC prevent tumor growth *in vivo*

(A) Groups of mice (n=5) were injected in the footpad with OVA257-264 (100 ng/ml) sorted pDC subsets (1×10^5/mouse) at days -14 and -7. At day 0, mice were challenged with EG7 tumor cells (0.1×10^6/mouse) on the flank, and tumor growth was assessed every other day. Circles: CD9^{pos} pDC, Squares: CD9^{neg} pDC, Triangles: PBS. (one-way ANOVA, P=0.006, F=7.252). (B) Tumor-draining and contralateral LN were dissected from individual mice and the numbers of infiltrating FoxP3+ CD4+T cells (Student's T-test, n=4, P=0.048) and FoxP3+CD4+Vα2+ T cells were determined. (+/− s.d). The data represent one of two experiments performed with similar results.

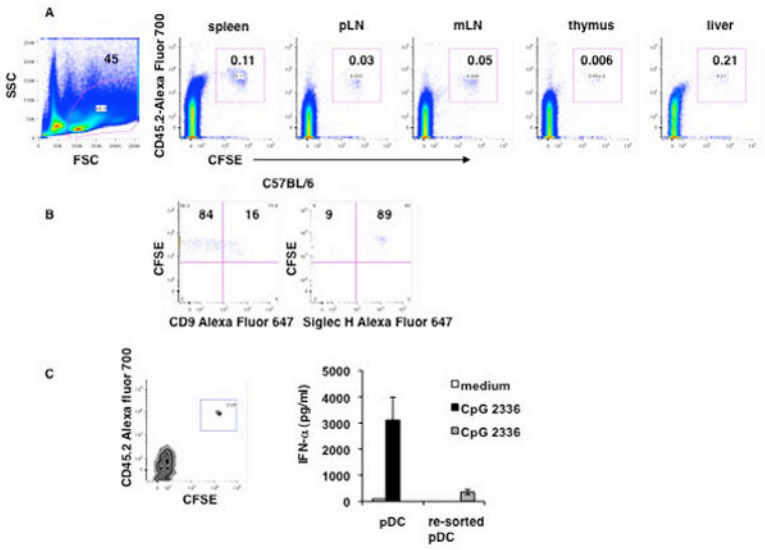

Figure 6. CD9^{pos} pDC differentiate into CD9^{neg} pDC *in vivo*

(A) CD9^{pos} pDC were sorted, CFSE-labeled and injected into congenic CD45.1 recipient mice. After 4 days, different tissues were harvested and analyzed for the presence of donor pDC. (B) FACS analysis of transferred CD9^{pos} pDC from the spleen of recipient mice. (C) Total CFSE-labeled pDC were transferred into congenic recipients and after 2 days, spleen and LN were harvested, pooled and donor cells were re-sorted based on their expression of CD45.2 and CFSE. Re-sorted pDC (5×10^4) were cultured in the presence of CpG 2336. Supernatants were harvested after 48 hours and analyzed for IFN-α. (two-tailed, unpaired Student's T-test, P=0.0471) (s.d). Data shown are representative of three independent experiments.

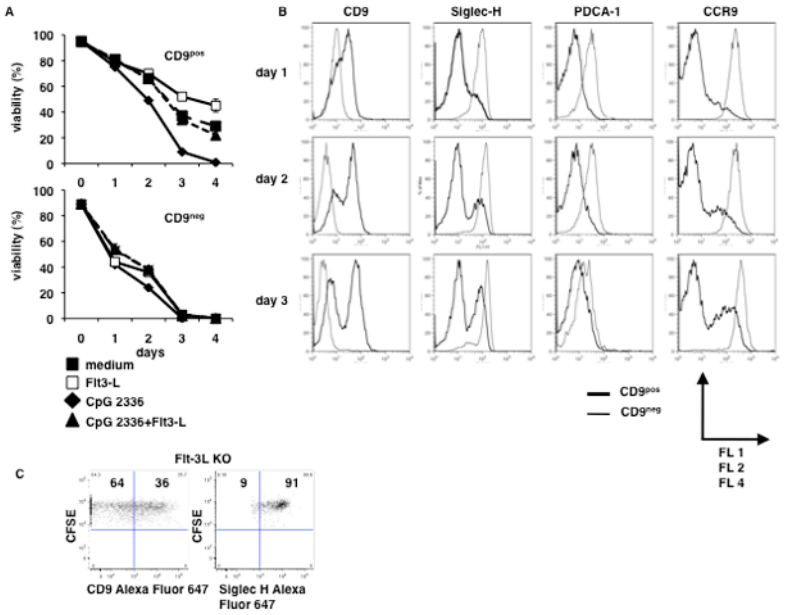

Figure 7. Flt3-Ligand promotes the viability of pDC subsets *in vitro*

(A) Sorted CD9^{pos} and CD9^{neg} pDC subsets were cultured for 4 days in medium alone (closed squares) or the presence of Flt3-L (open squares), CpG2336 (diamonds) or a combination thereof (triangles). Viability was determined by flow cytometry. One out of three similar experiments is shown. (s.d). (B) Phenotypic analysis of sorted subsets cultured in the presence of Flt3-L (*n*=3, Student's T-test, *P*=0.0487). (C) CFSE-labeled pDC from CD45.1 mice were injected into Flt3-L−/− recipients, and harvested from the spleens after 48 hours. Data are representative of four independent experiments.